

Search for Hidden photons with Sumico

Yoshizumi Inoue¹, Tetsuya Mizumoto², Ryosuke Ohta¹, Tomoki Horie¹, Jun'ya Suzuki¹, Makoto Minowa¹ (the Sumico collaboration)

¹The University of Tokyo, Japan

²Kyoto University, Japan

DOI: http://dx.doi.org/10.3204/DESY-PROC-2013-04/inoue_yoshizumi

We searched for solar hidden photons in the visible photon energy range using a hidden photon detector add-on attached to Sumico. It consists of a parabolic mirror of $\phi 0.5\text{ m}$ and $f = 1\text{ m}$ installed in a vacuum chamber, and a low noise photomultiplier tube at the focal point. No evidence for the existence of hidden photons was found in the latest measurement giving a new limit on the photon-hidden photon mixing parameter in the hidden photon mass range $0.001\text{--}1\text{ eV}$.

1 Introduction

The sun can be a powerful source of weakly interacting light particles, such as the axions [1, 2]. The Tokyo axion helioscope, aka. Sumico [3, 4, 5, 6], was built aiming at the direct detection of the solar axions in the mass range up to a few eV. It is equipped with a dedicated cryogen-free superconducting magnet which can produce a transverse magnetic field of 4 T over 2.3 m, a container to hold cold ${}^4\text{He}$ gas, a PIN-photodiode-array X-ray detector, and a telescope mount mechanism to track the sun. The transverse magnetic field is essential in the axion helioscope, where the solar axions oscillate into X-ray photons. In the past measurements, the axion mass ranges $0\text{--}0.27\text{ eV}$ and $0.84\text{--}1\text{ eV}$ have been scanned. We were striving to push up the sensitive mass range to higher masses. Unfortunately, however, axion search activity is currently suspended due to a trouble in the cryogenic system which is preventing the magnet from exciting. Meanwhile, we searched for solar hidden photons using Sumico.

The hidden photon is the gauge boson of a hypothetical hidden local U(1) symmetry. Many extensions of the standard model, in particular those based on string theory, predict such symmetries [7]. The hidden photon can couple to the ordinary photons via a so-called *kinetic mixing*, and it can be massive as described by the following Lagrangian [8, 9, 10],

$$\mathcal{L} = -\frac{1}{4}F_{\mu\nu}F^{\mu\nu} - \frac{1}{4}B_{\mu\nu}B^{\mu\nu} - \frac{\chi}{2}F_{\mu\nu}B^{\mu\nu} + \frac{m_{\gamma'}}{2}B_\mu B^\mu,$$

where $F_{\mu\nu}$ and $B_{\mu\nu}$ represent the ordinary- and hidden- photon field strengths, respectively, χ is the kinetic mixing parameter, and $m_{\gamma'}$ is the hidden photon mass. When the hidden photon has a small mass, it leads to photon-hidden-photon vacuum oscillations. In vacuum, hidden photon to photon transition probability for photons of energy ω after traveling ℓ is given by:

$$P_{\gamma' \rightarrow \gamma} = 4\chi^2 \sin^2 \left(\frac{m_{\gamma'}^2 \ell}{4\omega} \right)$$

assuming $m_{\gamma'} \ll \omega$. Since the refractive index for visible light in the matter is normally larger than 1, the matter in the conversion path always affects the transition probability negatively.

The emission of hidden photons from the sun was discussed by J. Redondo [11]. The transverse hidden photon flux at the earth is given by:

$$\frac{d\Phi_T}{d\omega} = \int_0^{R_\odot} \frac{r^2 dr}{(1 \text{ AU})^2} \frac{\omega^2}{\pi^2} \frac{\Gamma}{e^{\omega/T} - 1} \frac{\chi^2 m_{\gamma'}^4}{(m_\gamma^2 - m_{\gamma'}^2)^2 + (\omega\Gamma)^2},$$

where R_\odot is the solar radius, T is the temperature, Γ is the damping rate of photons, and m_γ is the effective photon mass in plasma. For $m_{\gamma'} \ll 1 \text{ eV}$, one can use the following conservative estimate for the bulk component of the hidden photon flux [11]:

$$\frac{d\Phi_T}{d\omega} \gtrsim \chi^2 \left(\frac{m_{\gamma'}}{\text{eV}} \right)^4 10^{32} \frac{1}{\text{eV cm}^2 \text{s}} \quad \text{for } \omega = 1\text{--}5 \text{ eV}.$$

Recently, a refined estimation including the contribution from a thin resonant region below the photosphere is given [12, 13] for four typical cases $m_{\gamma'} = 0, 0.01, 0.1$ and 1 eV . They claim that the resonant production dominates over the emission from the rest of the sun.

In more recent studies [14, 15], the estimated emission rate of longitudinal hidden photons was revised and it turned out that the resonant longitudinal-mode production is dominating the total solar hidden photon emission in the low mass case $m_{\gamma'} < 1 \text{ eV}$. This result has nothing to do with the analysis of our experiment since longitudinal hidden photons do not oscillate into photons in vacuum. However, it has a strong impact on the hidden photon searches by providing stringent constraints on the hidden photon parameters along with their another work [16] in which they re-analyzed the published data of the XENON10 dark matter experiment.

Various constraints on the hidden photon parameters are summarized in Ref. [17].

In this paper, we report on a direct experimental search for the flux of solar hidden photons.

2 Experimental apparatus

Our solar hidden photon detector was built as an add-on unit mounted on Sumico, the Tokyo axion helioscope, as shown in Fig. 1. Sumico can track the sun with a driving range from -28° to 28° in altitudinal direction and 360° in azimuth. The overall tracking accuracy is better than 0.5 mrad in both directions, which is negligibly small for this measurement.

The solar hidden photon detector consists of a vacuum chamber, a parabolic mirror and a photomultiplier tube (PMT). The vacuum chamber holds the conversion region in vacuum to keep the hidden photon to photon conversion probability high enough. It is a cylinder made of 1.5-mm thick stainless steel plates with wrinkles on its side for the mechanical reinforcement. The inner diameter of the vacuum chamber is 567mm and its length is 1200mm. The parabolic mirror was used to collect the conversion photons to the PMT. It is made of aluminium deposited soda glass. Its diameter is 500 mm, the focal length is 1007 mm and the focal

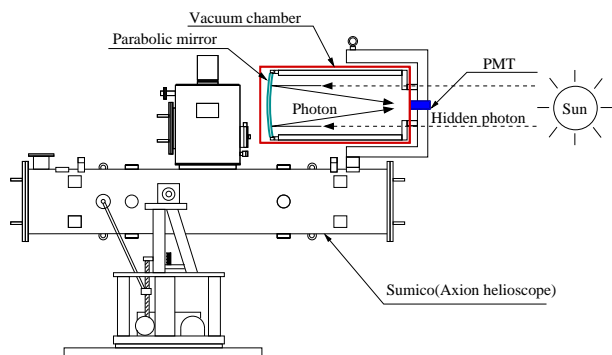


Figure 1: The schematic view of Sumico and the solar hidden photon detector.

spot diameter is 1.5 mm. The reflectance measured by the manufacturer is higher than 80% over the wavelength range 300–650 nm. The mirror and its supporting structure is constructed inside the vacuum chamber.

A low noise head-on type 25-mm diameter photon counting PMT, Hamamatsu Photonics R3550P, was used as the photon detector at the focal point. It is sensitive to photons of wavelength range 300–650 nm with a peak quantum efficiency of 17 %. It is set at the atmospheric pressure side and is viewing the reflected photons through a quartz glass window. Single- and multi photon events detected by the PMT make current pulses which enter a charge-sensitive preamplifier (ORTEC 113) and a shaping amplifier (ORTEC 572). The signal is then digitized by an ADC (Laboratory Equipment Corp. 2201A) and pulse height spectra are taken by a multichannel analyser (MCA).

The temperatures of the PMT and the vacuum chamber are measured by Pt100 thermometers. The inner pressure of the vacuum chamber is measured by a vacuum gauge (Balzers PKR250). During the solar tracking- and background measurements, the inner pressure of the vacuum chamber was lower than $(5 \pm 2) \times 10^{-3}$ Pa. The effect of this residual gas on the conversion probability is negligible.

3 Measurement and analysis

If a hidden photon is converted into a photon in the vacuum chamber, it would be detected by the PMT as a single photon event. Before starting the measurement, the shape of a single photon spectrum in the MCA was measured by illuminating the PMT with a blue LED with sufficiently low current pulses. It was fitted by a Gaussian function which was later used as the template for the single photon analysis.

Measurements were done from October 26, 2010 till November 16, 2010. The solar tracking measurements were done around the time of sunrise and sunset with tracking time of about 5 hours each. Background was measured while the detector was directed away from the sun.

To find out the possible evidence of solar hidden photons, the background spectrum was subtracted from the solar tracking spectrum. We must eliminate some systematic effects which have nothing to do with the solar hidden photons. It is well known that the dark count rate gets lower as time passes after an operating voltage is applied. We, therefore, waited for four

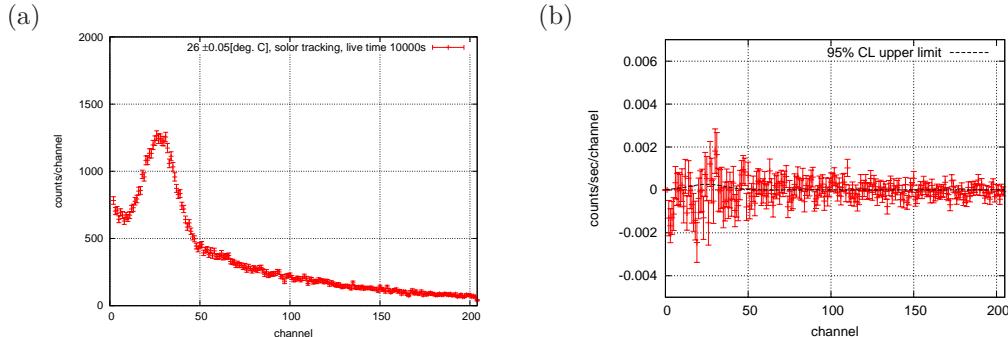


Figure 2: (a) An example of a pulse height spectrum (PMT temperature $26.0 \pm 0.05^\circ\text{C}$, solar tracking data). (b) Total residual spectrum and the 95% confidence level upper limit.

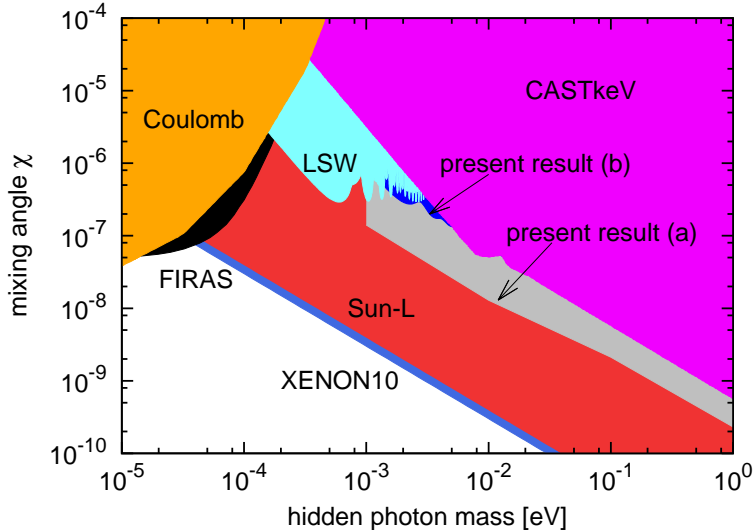


Figure 3: 95 % Confidence level upper limits to the mixing parameter χ set by this experiment. Present result (a) is obtained based on the the newer solar hidden photon flux calculation [12, 13] and (b) on the older conservative estimation [11]. Excluded area by other experiments are; Coulomb: tests of Coulomb's law [18, 19], LSW: Light Shining through Walls experiments [20, 21, 22, 23], CAST keV: the CAST experiment [11], FIRAS: FIRAS CMB spectrum [24], Sun-L: the solar luminosity constraints in the longitudinal channel [14, 15], and XENON10: interpretation of the XENON10 result in view of the longitudinal solar hidden photons [16].

days until the time dependence on the dark count rate became negligible.

To avoid the systematic effect from a temperature dependence of the dark count rate, we subtracted background isothermally. First, we grouped the solar tracking- and background-spectra each with 100s of live time into 21 temperature bins of 0.1°C interval whose central values ranging $25.9\text{--}27.9^\circ\text{C}$. Then, we apply the background subtraction within every temperature bin and obtained 21 residual spectra. Finally, the total residual spectrum was obtained by combining them.

In the above procedure, we used only the data during the holidays when the air conditioning system was switched off, because we observed abrupt room temperature changes on weekdays due to automatic switching of the air conditioning system of the building.

Figure 2 (a) shows the pulse height spectrum from solar tracking data in the temperature bin $26.0 \pm 0.05^\circ\text{C}$, as an example. Figure 2 (b) shows the total residual spectrum. It is worth noting that the peak from single photon events is already evident in the background spectrum and it vanished away after the background subtraction.

We then estimated how many single photons could there be in the total residual spectrum by fitting the magnitude of the Gaussian template function to it. The best fit was obtained with

$$N_{\text{fit}} = (-7.9 \pm 6.5(\text{stat.}) \pm 3.4(\text{sys.})) \times 10^{-3} [\text{s}^{-1}].$$

The systematic errors considered include an effect of Cherenkov light emitted in the quartz

glass vacuum window and the PMT window by cosmic muons, the finite bin width of the PMT temperatures, and the residual drift of the dark count rate after four days.

As we observed no excess of the single photon events, the 95% confidence level upper limit to the hidden photon counting rate was estimated taking the statistical and systematic errors into account:

$$N_{\text{UL95}} = 1.02 \times 10^{-2} \text{s}^{-1}.$$

The upper limit N_{UL95} is now compared with the count rate expected by the hidden photon model with given parameters. The 95% confidence level upper limit to the mixing parameter χ as a function of the hidden photon mass $m_{\gamma'}$ is calculated as shown in Fig. 3. For the solar hidden photon flux $\frac{d\Phi_T}{d\omega}$, two cases were assumed. One is based on the conservative estimation [11] which is indicated by ‘present result (b)’ in Fig. 3. The other is based on the newer estimation [12, 13] including the contribution from a thin resonant region below the photosphere, which is indicated by (a). Limits set by other experiments are also shown.

4 Conclusion and prospects

We have searched for solar hidden photons in the visible photon energy range using a dedicated detector for the first time. The detector was attached to the Tokyo axion helioscope, Sumico which has a mechanism to track the sun. No evidence of the existence of hidden photons is observed in the measurement and we set a limit on photon-hidden-photon mixing parameter χ depending on the hidden photon mass $m_{\gamma'}$. The present result improved the existing limits given by the LSW experiments and the CAST experiment in the hidden photon mass region between 10^{-3} and 1 eV. With recent new calculations of the longitudinal-mode hidden photon, more stringent limits came out by the solar luminosity consideration and also by the re-analysis of the XENON10 data. This result is already published in Ref. [25].

If solar tracking- and background measurements could be switched in less than 10 minutes, the effect of the dark-count-rate drift including that caused by the temperature changes would become negligible. This can be achieved by slightly switching the helioscope axis as much as 2 degrees while Sumico is tracking the sun. A test has demonstrated that Sumico can switch between the on-axis solar tracking and off-axis tracking within 20 seconds with enough direction accuracy. Use of a parabolic mirror of larger area and a photodetector with lower noise and higher quantum efficiency will also improve the sensitivity. However, such upgrades would not improve the sensitivity in terms of χ by orders of magnitude.

Acknowledgements

This research is supported by the Grant-in-Aid for challenging Exploratory Research by MEXT, Japan, and by the Research Center for the Early Universe, School of Science, the University of Tokyo.

References

- [1] R. Peccei, H. Quinn, Phys. Rev. Lett. **38**, 1440 (1977).
- [2] R. Peccei, H. Quinn, Phys. Rev. D **16**, 1791 (1977).

- [3] R. Ohta, *et al.*, Nucl. Instr. Meth. A **670**, 73 (2012).
- [4] S. Moriyama, *et al.*, Phys. Lett. B **434**, 147 (1998).
- [5] Y. Inoue, *et al.*, Phys. Lett. B **536**, 18 (2002).
- [6] Y. Inoue, *et al.*, Phys. Lett. B **668** 93 (2008).
- [7] M. Goodsell and A. Ringwald, Fortsch. Phys. **58**, 716 (2010).
- [8] L. Okun, Sov. Phys. JETP **56**, 502 (1982).
- [9] B. Holdom, Phys. Lett. B **166**, 196 (1986).
- [10] R. Foot, X. He, Phys. Lett. B **267**, 509 (1991).
- [11] J. Redondo, JCAP **07**, 008 (2008) [arXiv:0801.1527 [hep-ph]], S. N. Gninenko and J. Redondo, Phys. Lett. B **664**, 180 (2008) [arXiv:0804.3736v1 [hep-ex]].
- [12] D. Cadamuro and J. Redondo, arXiv:1010.4689v1 [hep-ph].
- [13] J. Redondo, arXiv:1202.4932v1 [hep-ph].
- [14] H. An, M. Pospelov, J. Pradler, arXiv:1302.3884 [hep-ph].
- [15] J. Redondo, G. Raffelt, arXiv:1305.2920 [hep-ph].
- [16] H. An, M. Pospelov, J. Pradler, arXiv:1304.3461 [hep-ph].
- [17] J. Jaeckel, A. Ringwald, Annu. Rev. Nucl. Part. Sci. 2010.60:405 [arXiv:1002.0329v1 [hep-ph]].
- [18] E. Williams, J. Faller, H. A. Hill, Phys. Rev. Lett. **26**, 721 (1971).
- [19] D. F. Bartlett and S. Loegl, Phys. Rev. Lett. **61**, 2285 (1988).
- [20] K. Ehret *et al.* [ALPS Collaboration], Phys. Lett. B **689**, 149 (2010) [arXiv:1004.1313v1 [hep-ex]].
- [21] M. Fouche *et al.* [BMV Collaboration], Phys. Rev. D **78**, 032013 (2008) [arXiv:0808.2800v1 [hep-ex]].
- [22] M. Ahlers *et al.*, Phys. Rev. D **77**, 095001 (2008) [arXiv:0711.4991v1 [hep-ph]], A. S. Chou *et al.* [GammeV Collaboration], Phys. Rev. Lett. **100**, 080402 (2008) [arXiv:0710.3783 [hep-ex]].
- [23] A. Afanasev *et al.* [LIPSS Collaboration], Phys. Lett. B **679**, 317 (2009) [arXiv:0810.4189v1 [hep-ex]].
- [24] A. Mirizzi, J. Redondo and G. Sigl, JCAP **03**, 026 (2009) [arXiv:0901.0014[hep-ph]].
- [25] T. Mizumoto *et al.*, JCAP **07**, 013 (2013) [arXiv:1302.1000v3 [astro-ph.SR]].